Authors reply to reviewer RC2

General

RC2: The manuscript in its current form is approximately four pages long, excluding tables and figures. In several instances, I found it necessary to move back and forth between the manuscript, Appendix A, and Jensen and Hansen (2021) in order to understand the procedures being applied. Readers who are not already familiar with Jensen and Hansen (2021) may experience difficulty following the nodding process and the deconvolution approach used in this study.

Author: The first reviewer RC1 recommends the addition of a few more figures to support the presentation of the deconvolution process. I have therefore added two more figures shown below. See reply AC1.

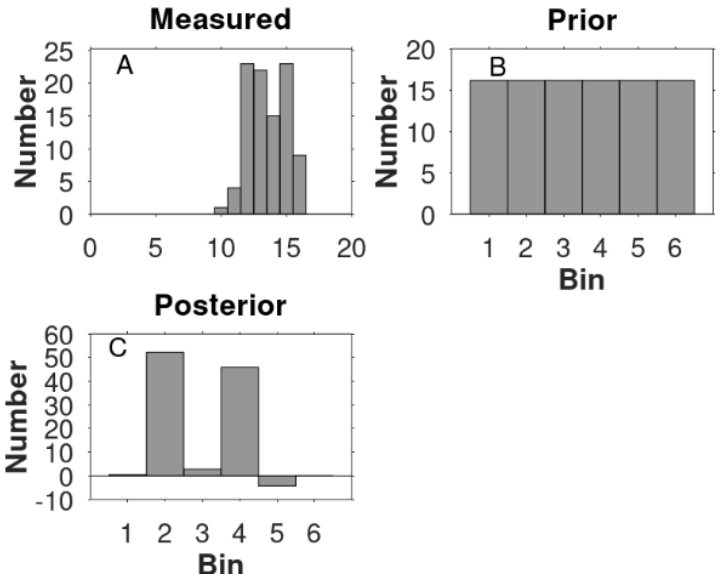

Figure A1: An example of vectors in Eq. (A24) shown as histograms. A. Fission track sample measurements $\boldsymbol{h}$. B. Prior information $\boldsymbol{h}_{prior}$ of the result of the inversion. The expected number of tracks is distributed equally over the bins. It is possible that all tracks are placed in a single bin but with low probability. C. The result of the deconvolution is the posterior $\tilde{\boldsymbol{h}}$ calculated by Eq. (A24).

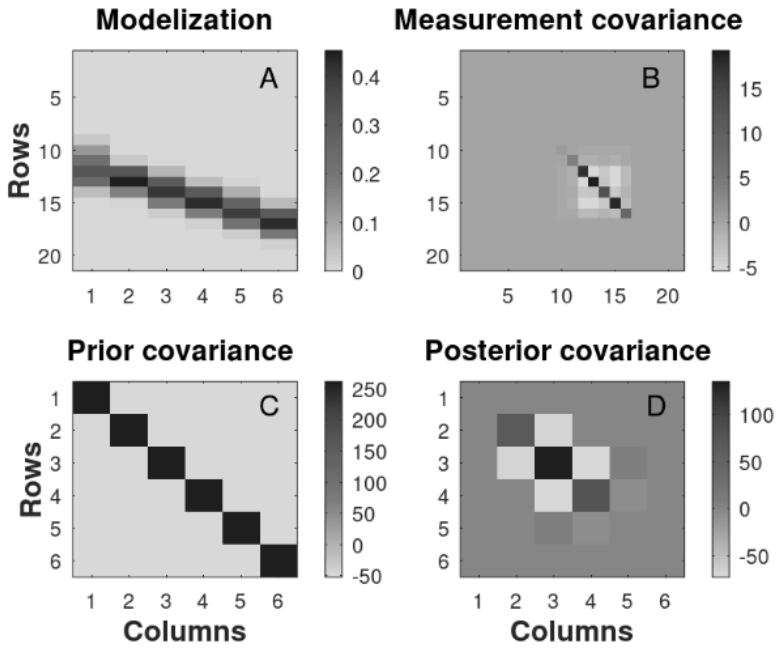

Figure A2: Maps of matrixes in Eq. (A24). The grayscale shows the number of tracks. A. The columns of matrix $\mathbf{G}$ are normalized histograms. The values are derived by interpolation among track length distributions measured in the laboratory. The track lengths are increasing along the rows, and the c-axis mean track lengths are increasing along the columns. B. Variance-covariance matrix $\mathbf{C}_H$ of the measurements. The diagonal values are the variances of the measurements calculated by Eq. (D1). The off-diagonal values are covariances of the measurements calculated by Eq. (D2). C. The prior variance-covariance values $\mathbf{C}_p$ are calculated by Eq. (D3) and Eq. (D4). The posterior variance-covariance $\mathbf{C}_p$ values are calculated by Eq. (A25).

RC2: In its present form, the manuscript resembles a short communication or technical note rather than a full research article. The author presents only three case studies based on data previously published in another study, and much of the methodological foundation appears to have already been described in Jensen and Hansen (2021).

Nevertheless, the approach itself is interesting and potentially valuable. The work could be suitable for publication; however, in my opinion, it would be appropriate for a short communication or a technical note.

Author: I agree. This paper describes three extensions relatively to Jensen and Hansen (2021): 1) The computer program is adapted to use c-axis projected tracks instead of mean track lengths. 2) Some equations have been updated to avoid approximations that are not necessary, and 3) several examples are run to show the robustness of the method. Five are now given in the paper and 20 more are shown in the Supplement.

RC2: The manuscript would benefit substantially if the author could expand the number of deconvolution examples using datasets from previously published studies. This would help demonstrate the broader applicability and robustness of the method.

Author: 25 deconvolution examples are given in the Supplement: https://doi.org/10.5281/zenodo.18062642, 2025a. I add two more examples in the manus.

Revision: In line 96: “The last example (Fig. 3) shows” → Figure 3 shows

The following is added at line 103:

Figure 4 shows an example with a histogram showing a pronounced peak. Forward calculation based on the deconvolved track length histogram does not mimic the details of the measurements. The track length distributions used in the deconvolution procedure do not show sharp peeks. These distributions are based on track length annealing experiments after a short time of radiation. The sample data are therefore insufficiently representing the thermal history of the sample.

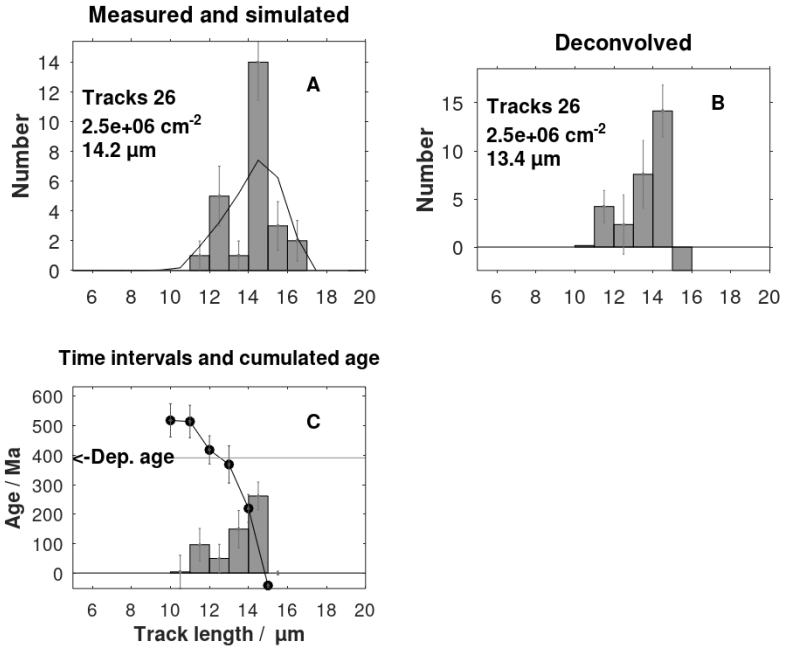

Figure 4: A. c-axis projected track histogram of the sandstone sample CXII-48 (Spiegel et al. 2023b) showing a poor simulation match to data probably caused by erroneous data. B. The deconvolution of the histogram shown in A. C. Time intervals and cumulated track ages, showing the presence of inherited tracks.

Figure 5 shows a skewed data histogram for a sandstone with inherited tracks. The cumulated ages shown in Fig. (5C) show the presence of inherited tracks. The c-axis projected tracks longer than 13 µm are post-depositional, Fig. (5D). The convolution (spreading out) of the deconvolved tracks, Fig. (5D), showing the part of the data histogram in Fig. (5A) that are expected to be of post-depositional origin.

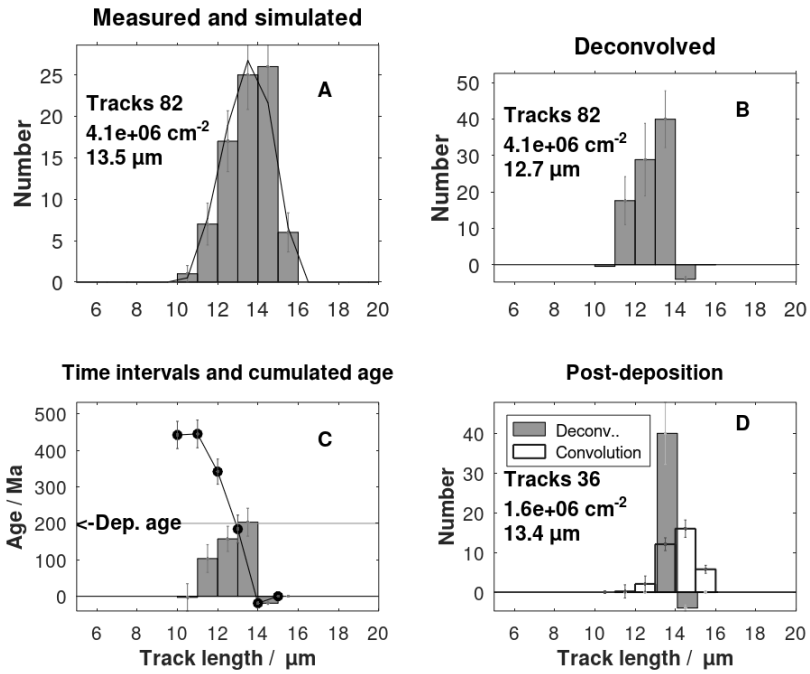

Figure 5. A. A skewed data c- axis projected track length histogram sample CXII-42 (Spiegel et al. 2023b). B. The deconvolved track length histogram. C. The sandstone deposition age is used to extract the post-depositional tracks shown in D. D. The deconvolved tracks together with the convolution hereof.

RC2: In addition, the etching of tracks in apatite is known to be anisotropic. Several factors, such as track thickness, the number of surface tracks intersecting a confined track, light source preferences during observation, and the targeted number of confined track length measurements, can influence the maximum and minimum lengths observed within a confined track length population. These aspects are not mentioned or discussed in the current manuscript. If the author considers these factors to be non-trivial, it would be valuable to address them in the discussion section.

Author: Thanks, these factors are non-trivial. It is important here to keep in mind that we are only interested in the relative distribution of the number of tracks related to length- not the absolute numbers. The diameter of etched tracks (1 micro meter?) connected to the surface is important for the number of fully included tracks being etched. The radius of the unetched track is much less, probably only a few Angstroms. The exact diameter of the etched track connected to the surface is therefore not important for the probability of long tracks intersecting the etched volume relatively to the short tracks.

The number of surface tracks intersecting a confined track is important for the absolute number but not for the relative number for the same reasons as given above.

The light source preferences during observation are probably important but I cannot comment on this since I have no experience with measuring tracks.

I am not sure of the meaning of “the influence the maximum and minimum lengths”. I think the meaning is the statistical importance of the number of tracks counted. If so, I can only agree.

Revision: The following is added to the discussion:

Several factors influence the number of tracks counted for a given track length bin. Important is the bias related to track length. Selection and measurement of track lengths are dependent on effect of light source preferences during observation which are not considered in the present mathematical development.

Line 17: Fission track age equations

Comment: The title of this section is “Fission track age equations”. Yet, there is only one equation given in the section.

Author: I agree.

Revision: “Fission track age equations” is replaced by “The fission track equation for age nodes”

Line 18: The traditional fission track age equation (Kohn et al., 2024)

Comment: 2024 is a bit too recent to be called traditional, I suppose. Which exact equation is being referred to here? It would be good to add this “traditional equation” in the text, maybe with slightly older reference, where it was first introduced.

Author: The first reviewer RC1 made a similar comment.

Revision:

Line 19: A commonly used equation to calculate the age of rapid cooling apatite minerals to temperatures below 60 °C is:

$$t = \frac{1}{\lambda_D} \ln\left(1 + \lambda_D \varsigma g \frac{\rho_s}{\rho_i} \rho_d\right), \quad (1)$$

where t is the age, λ_D is the total decay constant, ς is a calibration constant in accordance with age standards, g is the geometrical factor (0.5 for pi geometry, 1.0 for 4pi geometry), ρ_s is the surface track density, ρ_i is the induced fission track density, and ρ_d is the track density in the detector. See Hurford (2019) and Kohn et al. (2024) for a presentation of Eq. (1). The equation is based on earlier development e.g. Fleischer et al. (1975).

Line 22: … anneraling window from 120 C to 60 C…

Comment: Please add reference(s) for this.

Revision:

In line 27 “the partial annealing window from 120 °C to 60 °C” is replaced by

the partial annealing window from 120 °C to 60 °C (Gleadow, 1981).

Line 23: … included near horizontal fission tracks.

Comment: what is near horizontal? >10degrees? Or 15? Or whatever the analyst sees near horizontal?

Author: “Horizontal” means here that the tracks are in focus at both ends at the same time. As explained in Jensen and Hansen (2021) there is a depth window in which this can be the case. Short tracks are more likely to be accepted as being horizontal than long track according to this criterion.

Revision:

In line 24 the following sentence is added:

The criterion of being horizontal is here that the tracks are in focus at both ends at the same time (Gleadow et al., 1986b; Gleadow et al., 2019).

Line 26: The starting point is the randomly fully included oriented non-etched fission track in minerals….

Comment: I could not understand what was being said here.

Author: I hope the following enlightens:

Revision:

“The starting point is the randomly fully included oriented non-etched fission track in minerals caused by the natural fission of U-238.”

Is replaced in line 27 by:

Their mathematical development concerns the randomly oriented fully included fission track in minerals before they are made visible by etching. These latent tracks are caused by the natural fission of U-238.

Line 27: The tracks are generated through time, and the length is shortened as a function of time so that ideally the oldest tracks are the shortest ones and the more recent tracks are longest ones.

Comment: This would be partially true for unetched latent tracks in an isotropic system. The tracks are affected by the temperature through the time, the word temperature is missing in this sentence. If the author mentions apatites, the problem would be that this statement is not really right due to anisotropy. If this statement is on etched fission tracks, there are also some parts missing in this statement. How about the proximity to the surface and the number of intersecting tracks? They all contribute to the length.

Author: Thanks, “temperature” will be added. The tracks mentioned here are the undisturbed tracks before they are etched. Eq. (1) relies on the assumption that there is no anisotropy. I agree that anisotropy disturbs the statement about short tracks being older than longer tracks. This anisotropy contributes to the spreading of the observed etched tracks. This spreading (blurring) is taken care of by deconvolution as described in my paper.

Revision: The sentence

“They are generated through time, and the length is shortened as a function of time so that ideally the oldest tracks are the shortest ones and the more recent tracks are the longest ones.”

is replaced by:

The latent tracks are generated through time, and their lengths are shortened as a function of time and temperature. In apatite minerals the track lengths are shortened anisotropically contributing to a distribution of lengths. If we for a moment disregard the anisotropy and other blurring effects, it is expected that the oldest tracks are the shortest ones and the more recent tracks are the longest ones.

Line 36: Instead, it is therefore practice making them visible in the light microscope by etching (Kohn et al., 2024)

Comment: Etching is mentioned here for the first time. I assume the text on tracks discussed above are on latent tracks? The reader may easily get disconnected from the text flow.

Author: I agree, the word “latent” is now implemented a couple of places in the text above.

Line 39: Due to various biases and uncertainties (Ketcham, 2005) the observed track length histogram of etched tracks is blurred

Comment: Which biases and uncertainties?

Revision:

“Due to various biases and uncertainties (Ketcham, 2005) the observed track length histogram of etched tracks is blurred”

is replaced by:

Due to various biases and uncertainties, the observed track length histogram of etched tracks is blurred. Important factors are 1) the crystallographic biasing (Ketcham, 2003; 2005) causing distribution of track lengths as a function of angle to the c-axis, 2) the interpreters etching protocol and strategy for track selection (Ketcham, 2003).

Line 65: The columns of the deconvolved track length histogram (Fig. 1B) are converted to equivalent time intervals (Fig. 1C) using Eq. (A18).

Comment: Where is equation a18? It would be better to place it right here instead of making the reader wander through supplementary files.

Author: I see now it should not be Eq. A18 but Eq. A29 developed for a single time interval. It is now added as Eq. (2).

Revision: The sentence “The columns of the deconvolved track length histogram (Fig. 1B) are converted to equivalent time intervals (Fig. 1C) using Eq. (A18).”

is replaced by

The columns of the deconvolved track length histogram (Fig. 1B) are converted to equivalent time intervals (Fig. 1C) using

$$\Delta t^i = \frac{\sigma_s}{g\lambda_f c L_0} \frac{\tilde{\hbar}^i \sum_{j=1}^{M} (\frac{g_j^i}{\varkappa_j L_j})}{\sum_{i=1}^{N} \left(f(l^i) \tilde{\hbar}^i \sum_{j=1}^{M} (\frac{g_j^i}{\varkappa_j L_j}) \right)} \quad (2)$$

The development of the equation is given in Appendix A, where the equation is labeled Eq. (A29). Δt^i is the length of time interval i counting from the oldest to the most recent time interval, σ_s is the surface track density, g is the geometrical factor, λ_f is the track generation rate, c is the U-238 concentration, L_0 is the initial track length, $\tilde{\hbar}^i$ is the number of tracks generated in time interval Δt^i derived from the deconvolution procedure, $\sum_{j=1}^{M}$ is summation over all track length bins, g_j^i is the element of row j column i of matrix **G** given in Eq. (A22) in Appendix A. g_j^i is derived from interpolation among track length histograms based on laboratory annealing. $\varkappa_j$=1/L_j for tracks measured in translucent light and $\varkappa_j$=1 for measurements in reflected light, L_j is the centre of length binning j, $\sum_{i=1}^{N}$ is summation over the mean track bins, $f(l^i)$ is the function describing the relation between the relative surface track density to the relative mean track length (Eq. B1, Appendix B).

Equation 2 is used in the computer program but for future applications it is noted that for tracks measured in translucent light $\varkappa_j$=1/L_j and since the columns of matrix **G** are normalized $\sum_{j=1}^{M} g_j^i$ = 1 Eq. (2) condenses to:

$$\Delta t^i = \frac{\sigma_s}{g\lambda_f c L_0} \frac{\tilde{\hbar}^i}{\sum_{i=1}^{N} (f(l^i) \tilde{\hbar}^i)} \quad (3)$$

References (additional)

Gleadow, A. J. W.: Fission-track dating methods: What are the real alternatives?, Nuclear Tracks, 5,1–2, 3–14, https://doi .org /10 .1016 /0191 -278X(81)90021-4, 1981.

Gleadow, A. J. W., Duddy, I. R., Green, P. F., and Lovering, J. F.: Confined fission track lengths in apatite: a diagnostic tool for thermal history analysis, Contrib Mineral Petr, 94, 4, 405-415, doi:10.1007/BF00376334, 1986b.

Gleadow A., Kohn B., and Seiler C.: The Future of Fission-Track Thermochronology, in: Fission-Track Thermochronology and its Application to Geology, edited by Malusà M. and Fitzgerald P., Springer Textbooks in Earth Sciences, Geography and Environment, Springer, Cham, doi:10.1007/978-3-319-89421-8_4, 2019.

Hurford, A. J.: An Historical Perspective on Fission-Track Thermochronology, in: Fission-Track Thermochronology and its Application to Geology, edited by: Malusà M. and Fitzgerald P, Springer Textbooks in Earth Sciences, Geography and Environment, Springer, Cham., https://doi.org/10.1007/978-3-319-89421-8_3, 2019.